Journal of Atmospheric and Solar–Terrestrial Physics 252 (2023) 106134

Contents lists available at ScienceDirect

Journal of Atmospheric and Solar-Terrestrial Physics

journal homepage: www.elsevier.com/locate/jastp

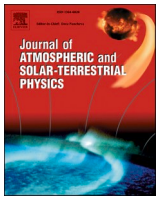

Research Paper

Impact of solar variability on Indian summer monsoon through large scale circulations

Vasundhara Barde [a], Aditi Upadhyay [a,c], Jayashree Bulusu [a], A.P. Dimri [a,b,*]

[a] Indian Institute of Geomagnetism, Mumbai, 410218, India
[b] School of Environmental Science, Jawaharlal Nehru University, New Delhi, 110067, India
[c] Johns Hopkins University Applied Physics Laboratory, Laurel, 20723, United States

ARTICLE INFO

Handling Editor: Dora Pancheva

Keywords:
Sunspot number
Indian summer monsoon
Large-scale circulation

ABSTRACT

Via large-scale circulations, the role of solar variability on the Indian summer monsoon is investigated. Standardized anomaly is used to identify years of solar maxima and minima. Statistical analysis such as moving mean, empirical mode decomposition, and wavelet analysis are used to determine the plausible relationship between solar variability, large scale circulations such as El- Niño 3.4 SST anomaly, Dipole Mode Index (DMI), and Atlantic Multidecadal Oscillation (AMO), and Indian summer monsoon rainfall (ISMR). In addition, the National Centers for Environmental Prediction/National Center for Atmospheric Research (NCEP-NCAR) reanalysis data collection is used to assess time-averaged composite anomalies of wind, latent heat, geopotential height during maximum/minimum solar activity years.

The 31-years moving mean of DMI shows significant negative correlation (−0.35) with sunspot number and with 31-years moving mean ISMR (−0.28). Similarly, 31-years moving mean of AMO exhibits a substantial positive connection with ISMR (0.68) and Niño 3.4 SST shows significant negative correlation (−0.62) with ISMR. Using intrusive mode function analyses it has noted that India receives rainfall for both phase of solar forcing but from wind studies at 850 hPa and 200 hPa, it is found that the phenomena for ISMR is different during solar maximum and minimum conditions. During solar maximum, a strong Low Level Jet is observed, and during solar minimum, a strong Tropical Easterly Jet is observed. Also, the area of influences of ISMR is different for solar maximum and solar minimum. The mean difference plot of seasonal rainfall shows that during solar maximum, north India receives reasonable amount of rainfall however during solar minimum, south India receives comparatively more rainfall than north India. A weakening of the local Hadley cell during solar minima is also observed.

1. Introduction

India is an agriculture based country and most of the population of rural India depends on agriculture and allied sectors. The Indian Summer Monsoon (ISM) accounts about 80% of the annual rainfall (Sahai et al., 2003), till date major agricultural activity in India depends on availability of rain water. ISM exhibit year to year variation in ISM Rainfall (ISMR) and also having variability at different temporal and spatial scale (Krishnamurthy and Krishnamurthy, 2014). ISM is a part of climate system and it's interaction with other component/process, viz., atmosphere-ocean-land-cryosphere, proves it to be a complex phenomenon. ISM affects and get affected by large-scale and local scale process, and because of this, higher order complexities are present for complete understanding of formation, onset, progression and dispassion of ISM.

Many studies have examined the variation in ISMR from year to year (Mohanty et al., 2005; Mishra et al., 2012; Walker et al., 2015; Barde et al., 2021; Maharana et al., 2021). During post-industrialization period, global warming became an important issue, and anthropogenic heating played a crucial role in monitoring, and potentially altering numerous weather processes and climatic variations. The combined study on impact of solar and anthropogenic forcing during 21st century has shown that solar forcing shows significant impact on earlier years of 21st century through temperature gradient, circulations and clouds, however anthropogenic impact is significant during recent years (Meehl et al., 2003). Thus, it is essential to analyses and comprehend the natural and anthropogenic modes of climate variability.

* Corresponding author. Indian Institute of Geomagnetism, Mumbai, 410218, India.
E-mail addresses: vasundhara.b@iigm.res.in (V. Barde), apdimri@hotmail.com (A.P. Dimri).

https://doi.org/10.1016/j.jastp.2023.106134
Received 24 May 2023; Received in revised form 4 September 2023; Accepted 9 September 2023
Available online 21 September 2023

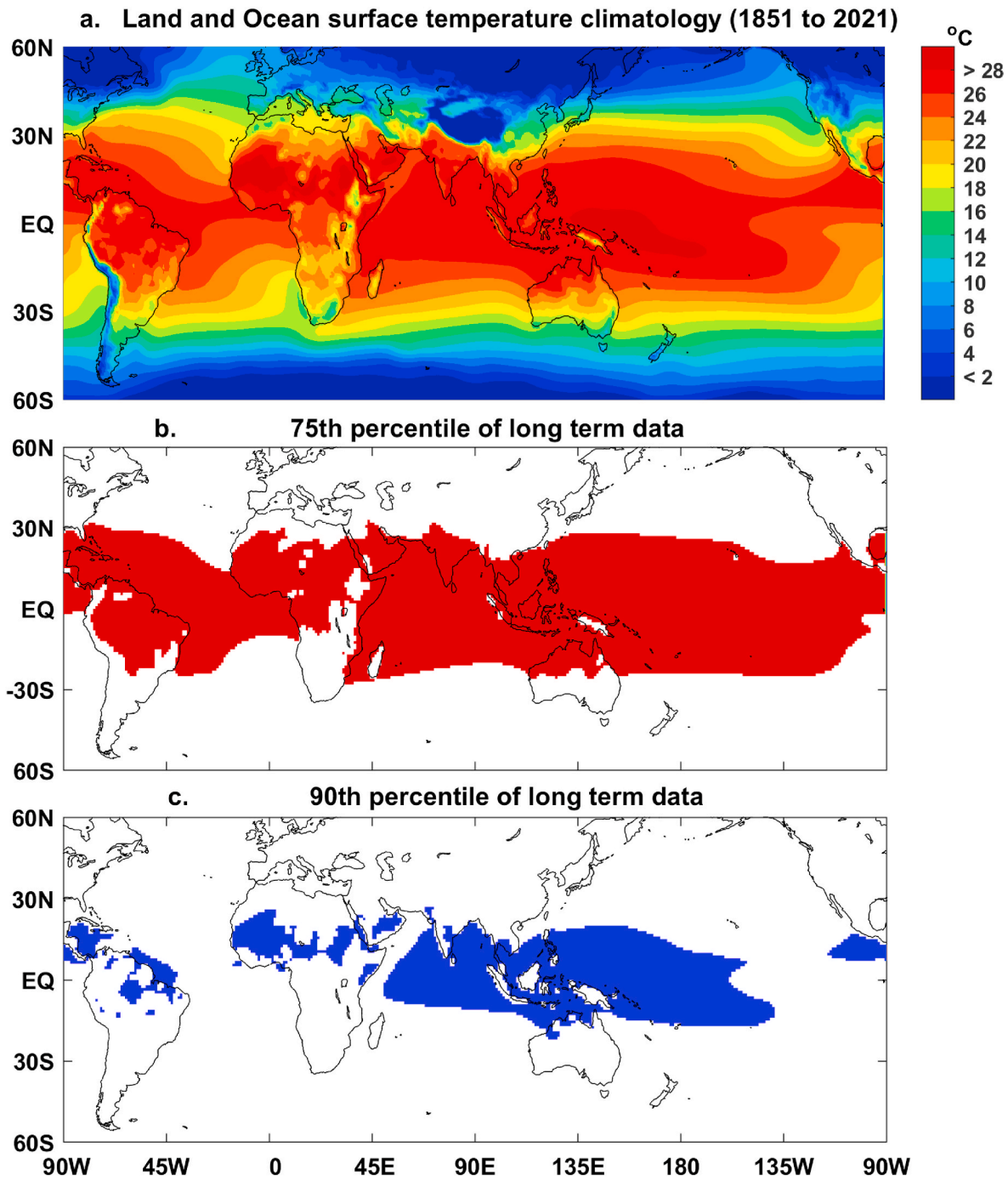

Fig. 1. Spatial pattern for the sea surface temperature, (a) long term mean by Berkeley Land and Ocean surface temperature (1851–2021) (b) 75th percentile of long term mean and (c) 90th percentile of long term mean by same data sets.

The Sun is the main energy source for the natural climate variations on Earth. Understanding the influence of solar forcing may be helpful in decadal and multidecadal climate forecasting. Knowing the impact of solar forcing can assist in decadal and multidecadal climate prediction. Previous researchers have explored the role of natural forcing in climatic variability (Hulme et al., 1999; Ghil, 2002; Solomon et al., 2011; Ghil and Lucarini, 2020). The Sun is G-type main sequence star and its magnetic activity and radiation intensities show fluctuation in cycles ranging from 11-years to more than 400 years. However the most dominant and relevant for studies in the Schwabe cycle, during which the sunspots number (represents the high magnetic activity of Sun) goes from a period of maxima to minima and maxima again over the course of 11 years (Hathaway, 2015). Impact of this 11-year solar cycle on climate variability has been discussed globally (Christoforou and Hameed, 1997; Haigh, 1999; Langematz et al., 2005; Meehl et al., 2009; Ineson et al., 2011; Chen and Zhou, 2012; Chiodo et al., 2019) also on the ISM (Hiremath and Mandi, 2004; Narasimha and Bhattacharyya, 2010; Ratnam et al., 2014). Gupta et al. (2005) mentioned that small changes in solar irradiance can bring pronounced changes in the tropical monsoon. The ISM is characterized by some semi-permanent features, such as Low Level Jet (LLJ) and Tropical Easterly Jet (TEJ), Ratnam et al. (2014) has shown that LLJ and TEJ get affected by solar cycle; they noticed a difference in magnitude of wind speed of about 2 m/s to 5 m/s for LLJ and TEJ respectively. Also, they noticed around 13 year's

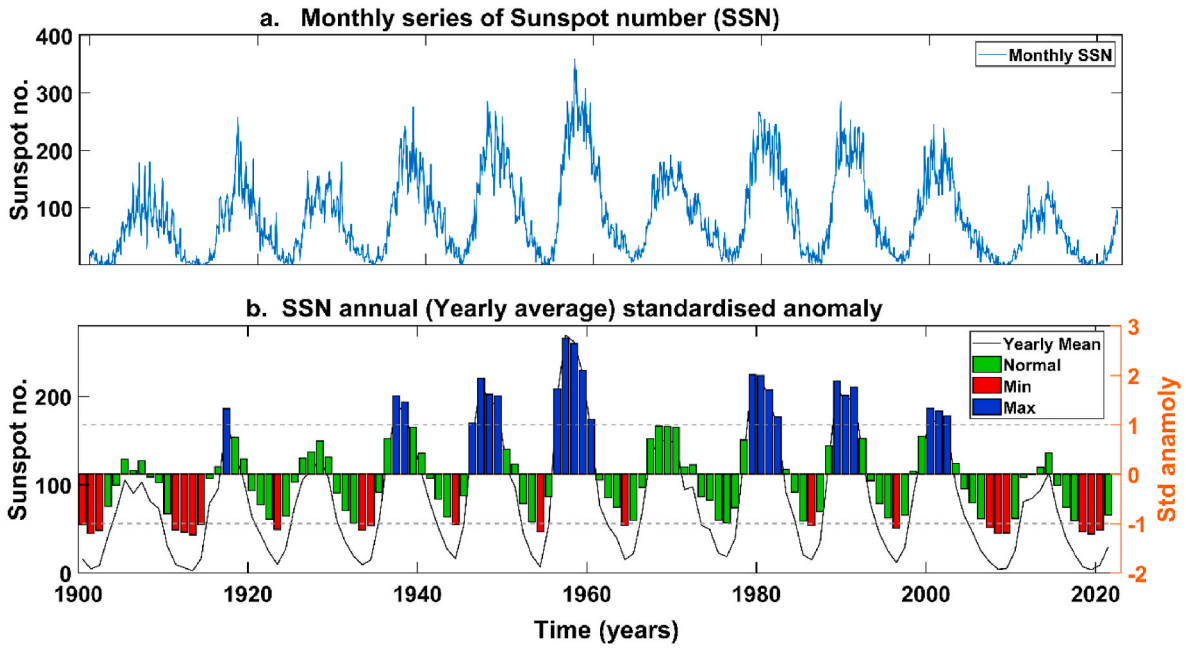

Fig. 2. Series of Sunspot numbers (SSN) (a) series of SSN using monthly data and (b) annual standardised sunspot anomaly.

Table 1
Sunspot cycle maxima, minima, ascending and descending years.

No.	Standardised Anomaly		Waldmeier/McKinnon (Hathaway, 2015)		Ascending years	Descending years
	Maxima	Minima	Maxima	Minima		
1	1917*	1901–1903	1907	1901	1902–1904	1908–1912
2	1937–1939*	1911–1914	1917	1913	1914–1916	1918–1922
3	1946–1949*	1923	1928	1923	1924–1927	1929–1932
4	1956–1960*	1933–1934	1937	1933	1934–1936	1938–1943
5	1968–1970	1944	1947	1944	1945–1946	1948–1953
6	1979–1982	1954	1957	1954	1955–1956	1958–1963
7	1989–1991*	1964	1968	1964	1965–1967	1969–1970
8	2000–2002*	1976	1979	1976	1977–1978	1973–1975
9	–	1986	1989	1986	1987–1988	1980–1985
10	–	1996	2000	1996	1997–1999	1992–1995
11	–	2007–2009**	2014	2008	2009–2013	2001–2007
12	–	2018–2020	–	–	–	2015–2018

(Note: The single star (*) represents La-Nina years i.e. cold phase of ENSO and double star (*) represents El-Lino years i.e. warm phase of ENSO).

delayed effect of solar activity on ISMR and noted the inverse relation between TEJ strength and Central India rainfall. During peaks of 11-years solar cycle, relatively high pressure anomalies over land and low pressure anomalies over the surrounded sea is observed and therefore stronger ISM witnessed (Van Loon and Meehl, 2012). Paleoclimatic studies also carried for the linkage between ISMR and SSN (Agnihotri et al., 2002; Gupta et al., 2013; Munz et al., 2017). Agnihotri et al. (2002) checked solar influence on the intensity of the Indian monsoon using a sediment core from the eastern Arabian Sea dating back to 1200 yrs, the ~60 years periodicity observed in instrumental rainfall data and Periodicities of 200 ± 20, 105 ± 15 and 60 ± 10 yrs are observed in the proxy records coinciding with those known for solar cycles.

Although the sun's short term oscillations (9, 13 and 27 days; 1.3, 5, 11 and 22 years) are well established, the analysis of the longer period oscillations are not totally understood (Hiremath et al., 2015). Apart from Sun, Ocean is also important for earth's climate, as it stores heat. Ocean-atmosphere interaction is another driver of natural climate variability. Ocean variability also exhibits prominent modes that can influence ISMR on various timescales; these include the El- Niño Southern Oscillation (ENSO), the Pacific Decadal Oscillation (PDO), the Atlantic Multidecadal Oscillations (AMO), and the Indian Ocean Dipole (IOD). Roy (2014) analyzed the role of sun in atmosphere-ocean coupling in the Pacific region. Past research has examined the relationship between the ISMR, ENSO, and PDO (Sikka, 1980; Ropelewski and Halpert, 1987; Webster and Yang, 1992; Ashok and Saji, 2007). The regression analysis has shown that the 11-years solar cycle modulates the occurrence frequencies El-Niño and La-Nina events in central pacific (Lin et al., 2021). Roy and Collins (2015) checked impact of solar activity on ENSO by using sea level pressure for 1850–2004 years, they found a strong sea level pressure signal around the Indian Ocean and it impacts via variations in the local Hadley circulation which further modulating the ISM. Moreover, they mentioned that results in that study also changed if the analysis period was different, the linkage for SSN and ISMR is valid before 1950 (Roy and Collins, 2015). Since 1970, the relationship between ISMR and ENSO is diminishing, and a relationship between the IOD and ISMR has also been seen (Kumar et al., 1999; Ashok et al., 2001; Mujumdar et al., 2007; Chakravorty et al., 2013). The IOD has emerged as one of the ISM modulators and is of vital importance in the ENSO-ISM relationship (Ashok et al., 2001).

Recent research indicates that the AMO influences the vertical wind anomaly in the Indian Ocean region via the multidecadal Atlantic–Indian Ocean teleconnection (Xie et al., 2021). To understand the impact of solar variability on ISMR variability, it is necessary to analyze solar variability and ISMR on multiple time scales ranging from short to long

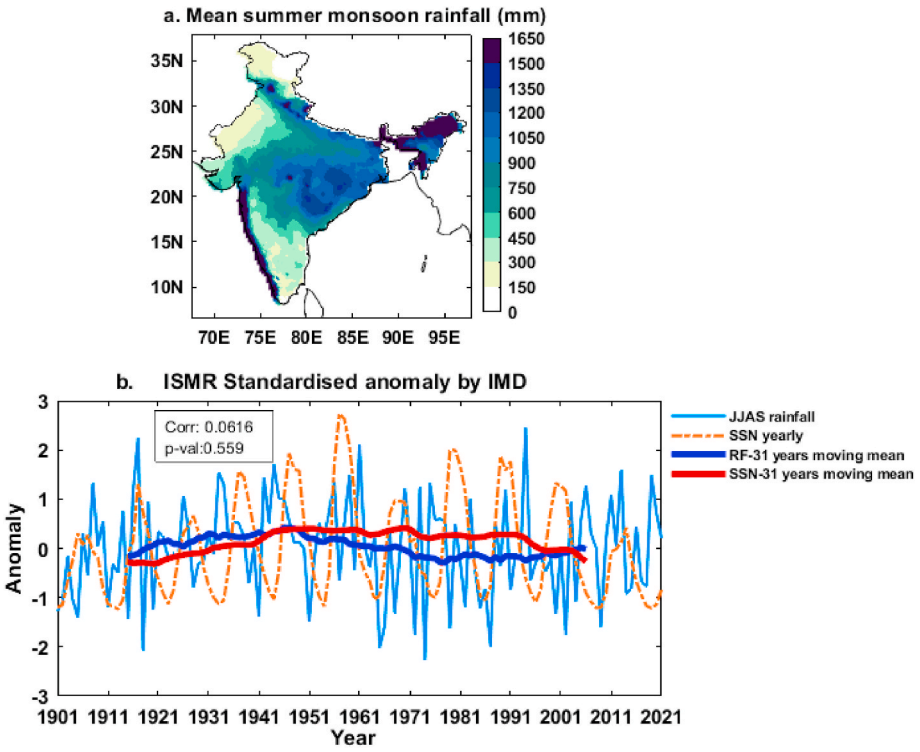

Fig. 3. Indian summer monsoon rainfall (ISMR) distribution, (a) long term mean spatial distribution by IMD gridded (1901–2021), (b) ISMR standardised anomaly by IMD gridded data (1901–2021). The correlation and *p*-value is calculated for the 31-years moving mean.

periods. Malik and Brönnimann (2018) employed excessive statistical analysis for AMO, PDO, Niño, Total Solar Irradiance (TSI), and ISMR for 146 years of observed data (1854–1999) and 399 years of atmosphere–ocean–chemistry climate model simulations (1600–1999); they observed that on an 11-year timescale, ISMR and TSI did not show any significant relationship. However, on multi-decadal timescales, the intrinsic negative correlation between ISMR and TSI is transformed into a statistically significant positive by AMO via changes in the summer (June to September; JJAS) meridional gradient of tropospheric temperatures. However, the role of AMO-IOD on ISMR is not considered in their study.

Thus, from the state of art of influence of solar activity on climate variability rests on the broad temporal scale of solar activity. It should be noted that the 11 year solar activity cycle itself is very different and involves different phases. The physics and the energy input to atmosphere varies from solar maximum to minimum (Van Loon et al., 2004; Solomon et al., 2011, 2019). Thus, different atmospheric processes may be supported during different phases of solar activity. This forms the central theme of this research. While the broad temporal relations are derived between sunspot numbers and compared with other studies, the contribution of years of solar maxima and minima are discussed in greater detail.

This paper presents a detailed examination of observed solar forcing on PDO, Niño 3.4 index, AMO, and IOD, as well as ISMR, so that the impact of solar variability on large-scale circulation and, consequently, ISMR can be understood. The ISMR is characterized by some semi-permanent features, such as LLJ and TEJ, in this study these two features are considered. Moreover, limited studies are available for the solar maxima, minima and their link to climate indices. Therefore, in this study, solar forcing in terms maximum/minimum sun spot activity and their influence on ISMR through large scale circulation is considered. The solar activity is measured by using the number of sunspots.

2. Data and methodology

The India Meteorological Department (IMD) gridded rainfall data (0.25° × 0.25°) for 121 years (1901–2021) during the ISM season is used. Rainfall distribution is well captured by this data set as preparation for this data set uses 6955 uniformly distributed rain-gauge stations (Pai et al., 2014). The IMD daily gridded rainfall dataset can be assess at https://www.imdpune.gov.in/cmpg/Griddata/Rainfall 1 NetCDF.html. The monthly mean data (u, v, vertical velocity, temperature) at various pressure levels along with the latent heat flux from the National Centers for Environmental Prediction/National Center for Atmospheric Research (NCEP/NCAR) reanalysis data set are used for large scale circulation analysis (Kalnay et al., 1996). The spatial resolution of the NCEP/NCAR data set is 2.5° × 2.5°.

The sunspot number monthly time series (1749–2022) was obtained from the Sunspot number (SSN) data that was provided by the World Data Center SILSO, Royal Observatory of Belgium, Brussels. The data set can be found on the website https://www.sidc.be/silso/datafiles. The monthly data are then transformed into a yearly dataset, and a standardized SSN series is generated for each year by following formula,

$$SSN\ Standardised\ anomaly = \frac{SSN_i - \overline{SSN}}{\sigma_{SSN}} \quad \text{Eq. (1)}$$

where, SSN_i is yearly value of SSN, $\overline{SSN}$ is long term mean and σ_{SSN} is standard deviation. The standardized sunspot anomaly mentioned in Eq. (1) has been used in previous research by Wang and Zhao (2012) and Chaudhuri et al. (2015). The ascending and descending years are Dipole Mode Index (DMI) used for IOD phase computation; the monthly DMI, Niño 3.4 index, PDO index, and AMO index may all be found at https://psl.noaa.gov/site_index.html. In order to breakdown yearly rainfall, AMO, SSN, PDO, and DMI values, an approach known as the Empirical Mode Decomposition (EMD) technique is implemented (Huang et al., 1998). EMD is a methodology that is data driven, it does not require a pre-determinant set of mathematical functions, and this method is

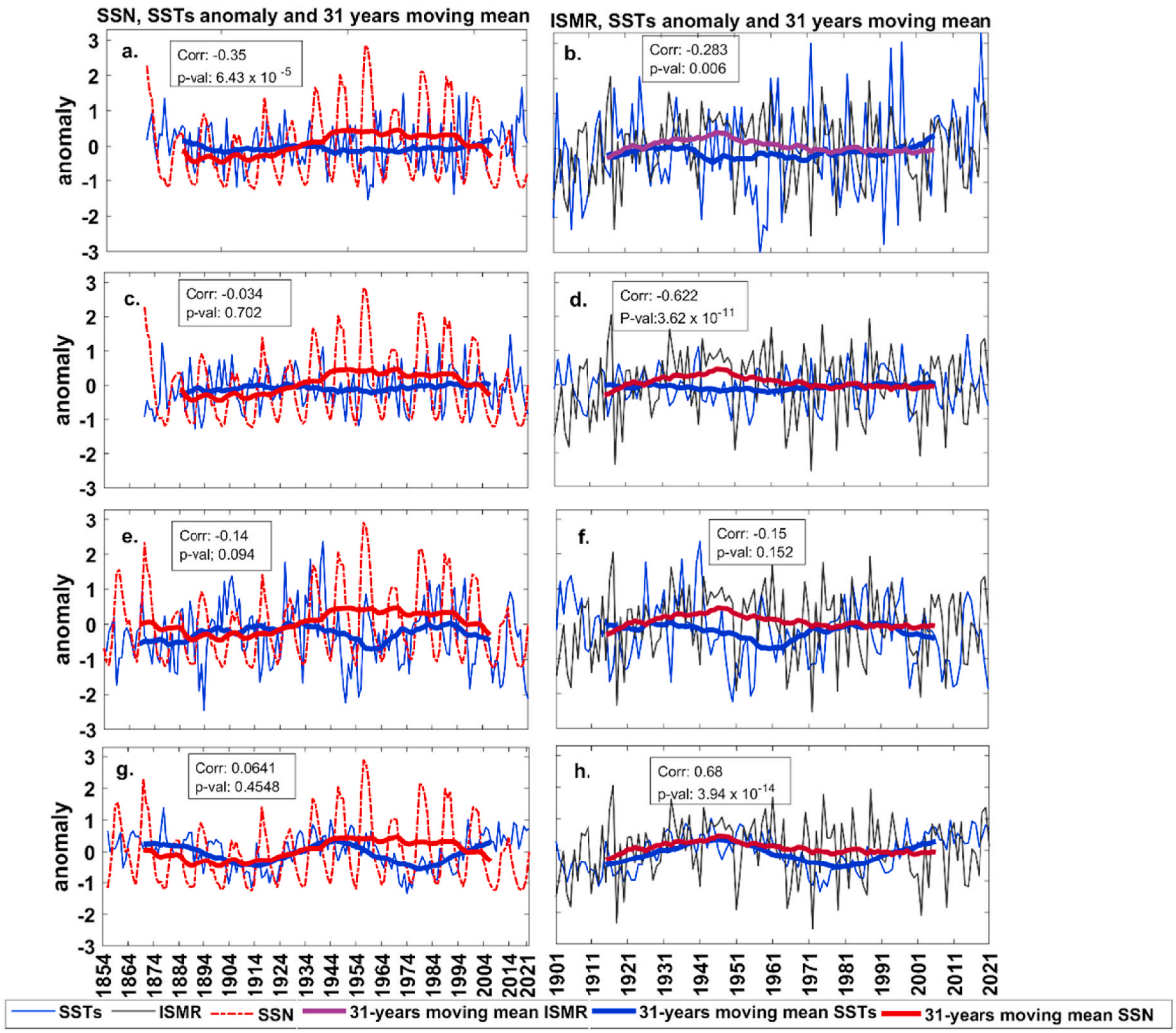

Fig. 4. Yearly time-series and 31-years moving mean inter-comparison between SSN with climate indices (a) DMI with SSN, (b) DMI with ISMR, (c) Nino 3.4 with SSN, (d) Nino 3.4 with ISMR (e) PDO with SSN (f) PDO with ISMR, (g) AMO with SSN and, (h) AMO with ISMR.

suitable for datasets that are non-stationary and non-linear, such as hydro climatology. EMD is an empirical, intuitive, direct, and adaptable method of decomposition in comparison to other decomposition methods (Wu et al., 2009). EMD algorithm decomposes a signal into intrinsic mode functions (IMFs) and a residual in an iterative process.

Maximum overlap discrete wavelet transform (MODWT) and Wavelet Coherence Analysis (WCA) is also calculated for AMO, DMI and SSN. Wavelet analysis can detect break points, trends, and discontinuities in time series that Fourier transforms may neglect (Rajaee and Shahabi, 2016; Kurths et al., 2019). There are two different kinds of wavelet transforms, the discrete wavelet transform (DWT) and the continuous wavelet transform (CWT). In this study DWT analysis take into consideration. Recently, wavelet coherence has emerged as a powerful tool for examining long-term relationships between hydro-climatological variables (Peters et al., 2004; Tan et al., 2016; Kurths et al., 2019). The MODWT is a modified DWT in which the subsampling process is left out. This gives the wavelet and scaling coefficients a higher level of information (when compared to the DWT). Even though the MODWT is harder to calculate than the DWT, it is not affected by shifts and can be used on time series with any sample size without any adjustments (Kurths et al., 2019). 31-years running correlation is carried out for Sea Surface Temperature (SST), SSN and ISMR.

Time averaged composite anomalies of for Latent heat flux (lhtfl), SST, wind pattern at 850 hPa, wind pattern at 200 hPa, and Hadley circulation during maximum/minimum solar activity years are analyzed. Steam function/rotational wind, velocity potential is also calculated for 200 hPa.

Wave activity flux is useful tool to identify the regions where stationary or migratory quasi-geostrophic wave disturbance packets are absorbed or emitted (Takaya and Nakamura, 2001). The accumulated energy (more purely, wave activity) is released in the form of a stationary wave-train by decaying of the circulation anomalies which are of high-amplitude. The geostrophic approximation is a simplification of the equations governing the horizontal components of velocity. It is valid when the largest terms in the equations of motion are those involving the Coriolis force and the pressure gradient. According to Helmholtz's decomposition theorem, any two-dimensional velocity vector 'V' can be decomposed into nondivergent (rotational) part and an irrotational (divergent or potential) part corresponding to a stream function (ψ) and a velocity potential (χ), respectively.

$$V = v_r + v_d \quad \text{Eq. (2)}$$

The rotational wind 'v_r' has all of the vorticity and no divergence and divergent wind 'v_d' has all of the divergence and no vorticity.

The student t-test is a statistical test used to compare the means of two groups. This method is used when comparison of mean of two series is take into consideration. The formula for the student-t test as follows,

$$t = \frac{\overline{x_1} - \overline{x_2}}{\sqrt{\left(\frac{1}{n1} + \frac{1}{n2}\right)}} \quad \text{Eq. (3)}$$

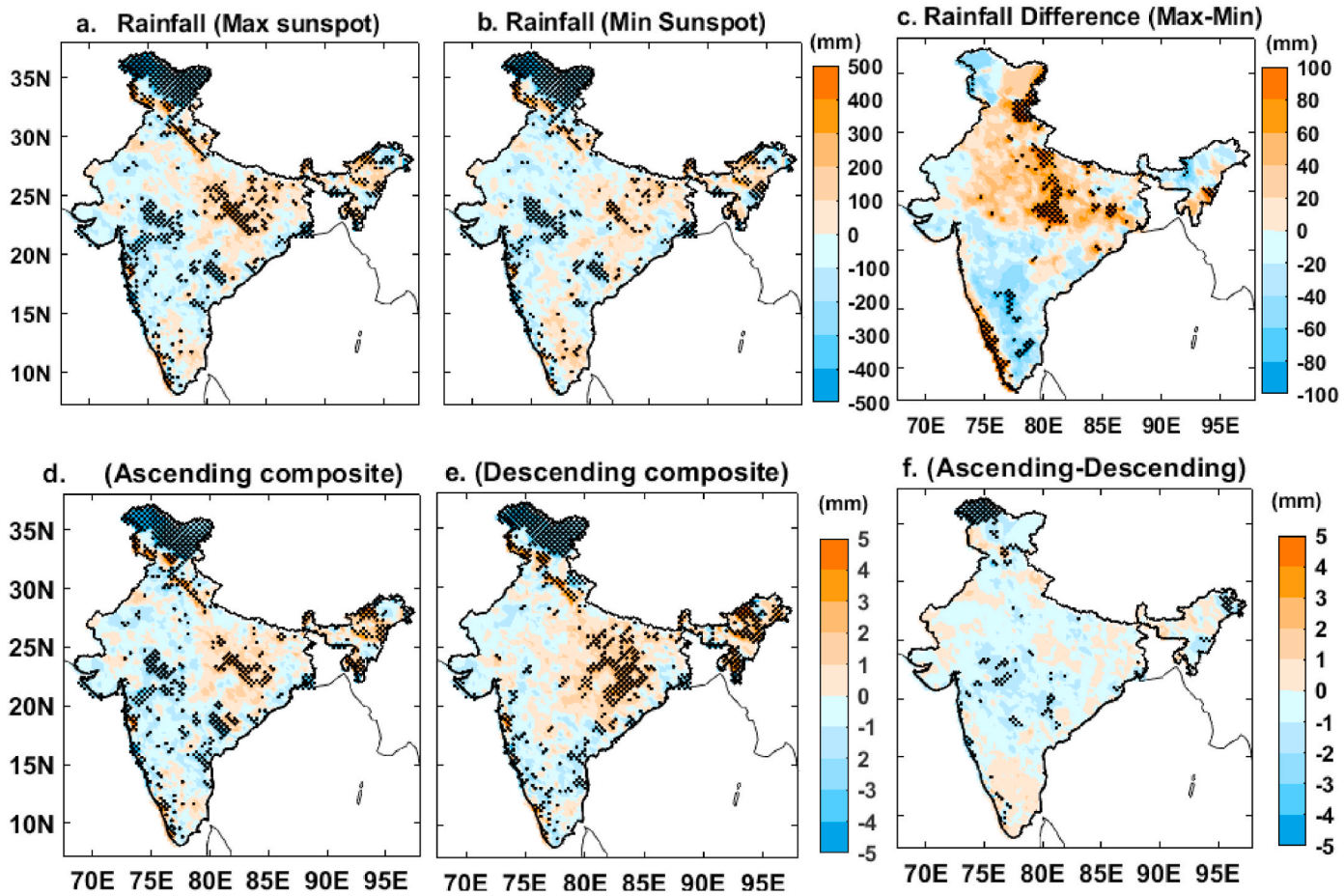

Fig. 5. Time average composite of seasonal rainfall (mm) anomalies during (a) Maximum sunspot years, (b) Minimum sunspot years, and (c) difference between maximum and minimum sunspot years; similarly rainfall distribution during (d) Ascending solar cycle years, (e) Descending solar cycle years and (f) difference between ascending and descending years. The dotted region shows the 95% confidence level.

In this formula, $\overline{x_1}$ and $\overline{x_2}$ are means of the two groups being compared, n_1 and n_2 are the number of observations in each of the groups. The significance of student-t test is checked using p-value. If a p-value less than 0.05 then result is statistically significant at 95% confidence level and result is insignificant if p-value is more than 0.05.

3. Results

3.1. Variation of SSN and ISMR

The spatial distribution of the climatology of annual temperature is depicted in Fig. 1a. Sun rays hit different parts of the planet's surface at different angles because the earth is spherical. The sun's rays are more intense and direct closer to the equator than they are further north or south. Most of the warmest condition occurs between 30°N and 30°S, where temperatures tend to hover around the 75th percentile (Fig. 1b). The region receives maximum (90th percentile) amount of solar energy is depicted in Fig. 1c. The region from Arabian Sea, Indonesian Sea to equatorial central Pacific Ocean come under the hottest SST regions (Fig. 1c) and this region is dominated by IOD and ENSO (Nino 3.4). Also, part of Indian land mass also come under hottest area, so impact of solar variability on ISMR through IOD seems justified.

The Monthly solar sunspot number are shown in Fig. 2a. The SSN after 1900 considered in this figure to match IMD rainfall data-set period. The yearly average SSN are considered for SSN Standardized anomaly calculation (Fig. 2b). Maximum sunspot number is shown by blue color, minimum is shown by red color and years in between ± 1σ (±1 Standard Deviation) considered as normal years, shown by green color. After 1960, number and intensity of maximum SSN years are decreased. The details of minimum/maximum sunspot number are given in Table 1. It is observed that most of the years of solar maxima are occurred during cold phase of ENSO.

There are similar type of studies available for linkage between SSN and influence natural climate variability indices for Africa and Europe, Lüdecke et al. (2021) analyzed the AMO, IOD, PDO, ENSO and SSN on 49 African countries rainfall, they showed that solar activity influences rainfall in a linear way in smaller-scale regions during certain seasons with extraordinary strength. Laurenz et al. (2019) found the positive correlation between precipitation and solar activity in central Europe, also, the variability is controlled by natural as well as anthropogenic factors.

3.2. Variation of SST with SSN as a controller of ISMR

Fig. 3a shows the spatial distribution of climatology for ISMR, the eastern India, north east India and Western Ghats receives more rainfall compare to other part of India. This spatial distribution of long-period average of seasonal rainfall over all India remains almost same however, year-to-year fluctuation in seasonal rainfall amount is observed (Fig. 3b). The standardized rainfall anomaly for ISMR and SSN standardized anomaly is presented in Fig. 3b, for climate change analysis roughly 30 years average is considered; therefore 31-years moving mean is considered to evaluate the correlation pattern. Also, in 31-years moving mean method, sun's short term oscillations i.e. 11-years, 22-years filtered out.

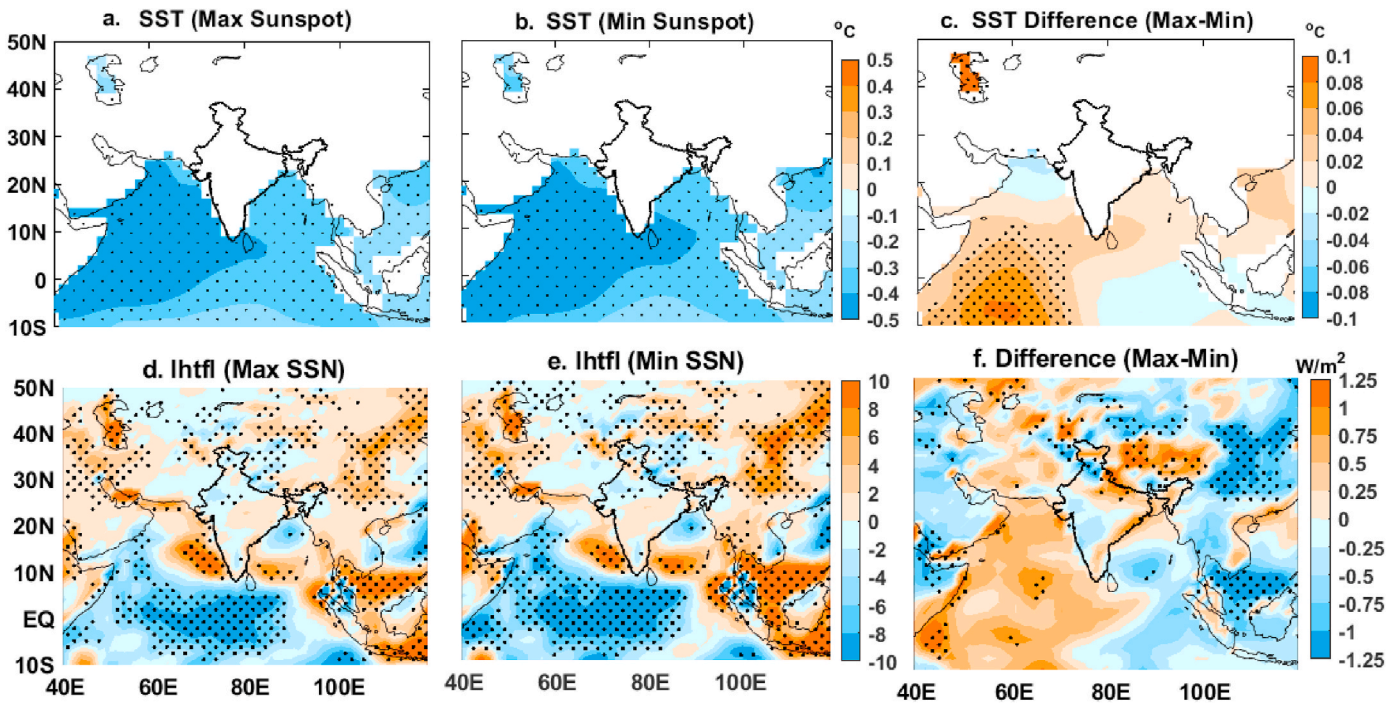

Fig. 6. Sea surface temperature (SST) composite for (a) Maximum sunspot years, (b) Minimum sunspot years, (c) difference between SSTs during maximum and minimum sunspot years; Similarly, Latent heat flux (lhtfl) composite for (d) Maximum sunspot years (e) Minimum sunspot years (f) same as (c) but only for lhtfl. The dotted region shows the 95% confidence level.

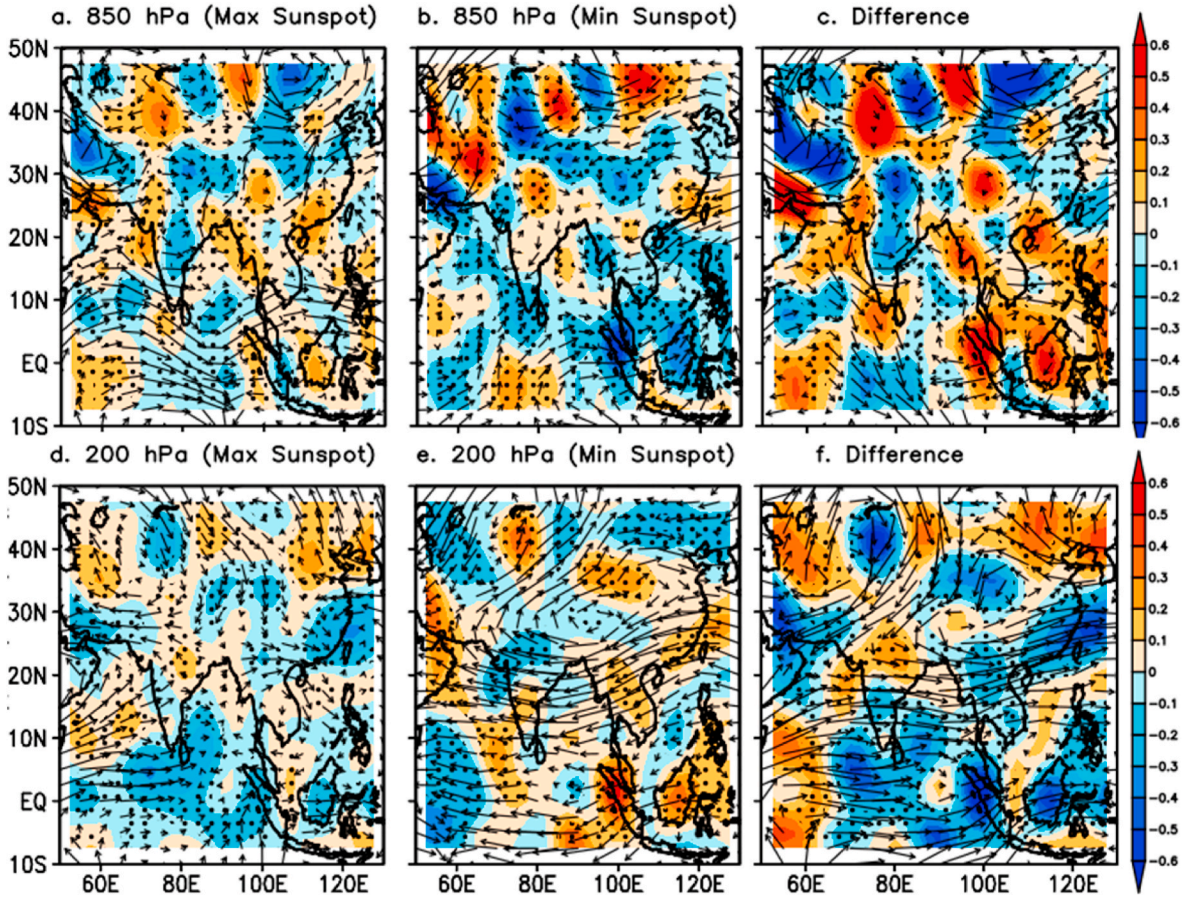

Fig. 7. Wind (ms^{-1}) composite at 850 hPa for (a) Maximum sunspot years (b) Minimum sunspot years and (c) difference between 850 hPa wind during maximum and minimum sunspot years; similarly wind composite at 200 hPa (d) Maximum sunspot years, (e) Minimum sunspot years and (f) same as (c) but only for 200 hPa wind. The dotted region shows the 95% confidence level.

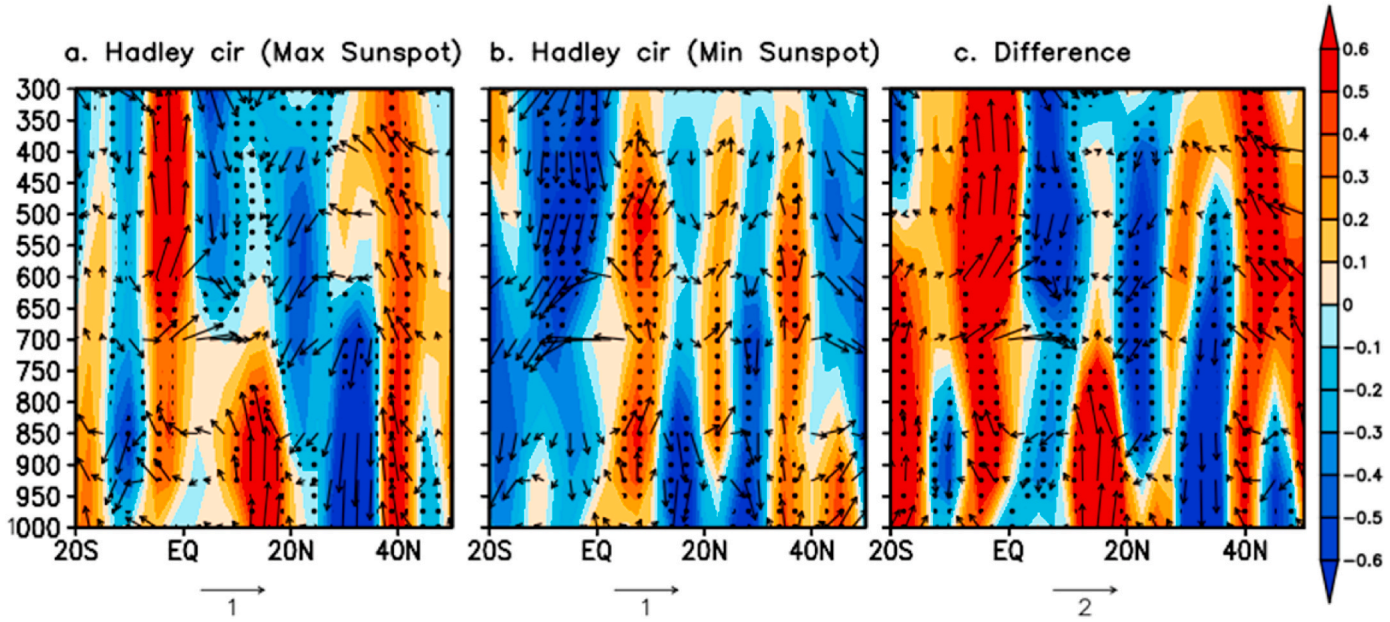

Fig. 8. Local Hadley circulation during (a) Maximum sunspot years (b) Minimum sunspot years and (c) Difference. The dotted region shows the 95% confidence level.

As a result, the further calculation makes use of the IMD gridded data. Fig. 4 depicts the annual variation of SSN and ISMR from two combinations, as well as the large scale index. The right panel compares the 31-years moving mean of SSN and large scale circulations, while the left panel compares the 31-years moving mean of ISMR and large scale circulation. Significant negative correlation (−0.35) exists between the DMI and SSN (Fig. 4a), similarly, significant negative correlation (−0.28) exists between the DMI and ISMR (Fig. 4b). There is no association between the Nino-3.4 SST index and SSN (Fig. 4c), although Nino-3.4 SST shows a significant negative correlation with ISMR (Fig. 4d). PDO does not correlate strongly with SSN or ISMR over 31-years moving mean correlation (Fig. 4e and f). AMO has a significantly positive correlation with ISMR but none with SSN (Fig. 4g and h). From the 31-years moving mean, during one long duration periodicity (not exactly but approximately 60 years) one peak and one trough is observed for SSN, and for the same time approximately two peaks and troughs are observed for 31-years moving mean of AMO (Fig. 4g). As previously stated, AMO also influences the vertical wind anomaly in the Indian Ocean (Xie et al., 2021).

The relationship between AMO, DMI, and ISMR required investigation. EMDs for AMO, DMI, and SSN are generated (Fig. S1). It is found that the decomposition component IMF-4 of AMO and DMI are relatively similar (Figs. S2a and S2b), as are IMF-5 of SSN and IMF-6 of DMI (Figs. S1b and S1c). This result supports the fact that IOD and ISMR regions are come under 90th percentile of surface temperature and therefore IOD shows delayed impact of SSN through IMF analysis. To examine the relationship between SSN and AMO, MODWT formulated, the 7th decomposition component, D7, and the long-term component, D8, as depicted in Fig S2. According to D7, the AMO and SSN exhibit opposite phase. Moreover, Wavelet coherence analysis is performed for SSN, AMO, and DMI (Fig. S3).

3.3. Variation of different atmospheric variables according to solar cycle

In order to determine the relationship between ISMR and SSN, the temporal average composite rainfall anomaly for maximum and minimum SSN years is depicted in Fig. 5a and b along with their significant difference (minimum and maximum) (Fig. 5c). During maximum SSN years, the positive rainfall anomaly over central India is more pronounced than during minimum SSN years (Fig. 5c), i.e. for both maximum and minimum SSN, central India exhibits the presence of a positive rainfall anomaly; however, the mechanism by which this anomaly occurs may be distinct. Similarly, Fig. 5d, e, 5f depicts the ISMR rainfall distribution for ascending and declining years and their difference respectively. The ascending years are years during transition of solar minima towards solar maxima and similarly, the descending years are the years during transition of solar maxima towards solar minima. The details of ascending and descending years are shown in Table 1. During years of maximum SSN, central-north India and the Western Ghats receive good amount of rainfall than other part of country, and during years minimum SSN southern India receives more precipitation than northern India (Fig. 5a). In the recent decades ISMR decreased over Indo-Gangetic Plains and increased over south India (Mishra et al., 2012; Barde et al., 2021). From Fig. 2 it is observed that since 2005 the negative phase of solar activity i.e. comparably less solar activity happens. This conditions supports the earlier finding that during solar minima south India receives comparatively good rainfall than north India.

In tropical region, SST gradient plays important role in defining ISMR (Lindzen and Nigam, 1987). The variability of monsoonal rainfall might be supposed to be determined by the SST distribution in Indian Ocean. Timed average composite of SST anomalies over Indian Ocean during maximum, minimum and difference (maximum minus minimum SSN years) with 90% significant shown in Fig. 6a, b and 6c respectively. During maxima and minimum SST is warmer in Arabian Sea (Fig. 6a and b), however, from the difference plot it is clearly seen that the Arabian Sea SST is more during minimum solar activity years (Fig. 6c). Warmer south-western Arabian Sea than SST near Indonesian coast is positive IOD condition and during positive IOD years central north India shows positive anomaly for ISMR (Mishra et al., 2012), which is commensurate in Fig. 5c. For radiate heating and cooling, the sensible and latent heat mainly contributes to the diabatic heating of atmosphere which are considered vital in driving the atmospheric circulation. The time average composite of latent heat flux anomalies is shown in Fig. 6d, e, 6f for maximum, minimum SSN and their difference respectively. The presence of latent heat flux during maximum SSN activity (Fig. 6b) indicted more released of latent heat flux over Arabian Sea. There is sufficient evaporation from Arabian Sea and land, which result in

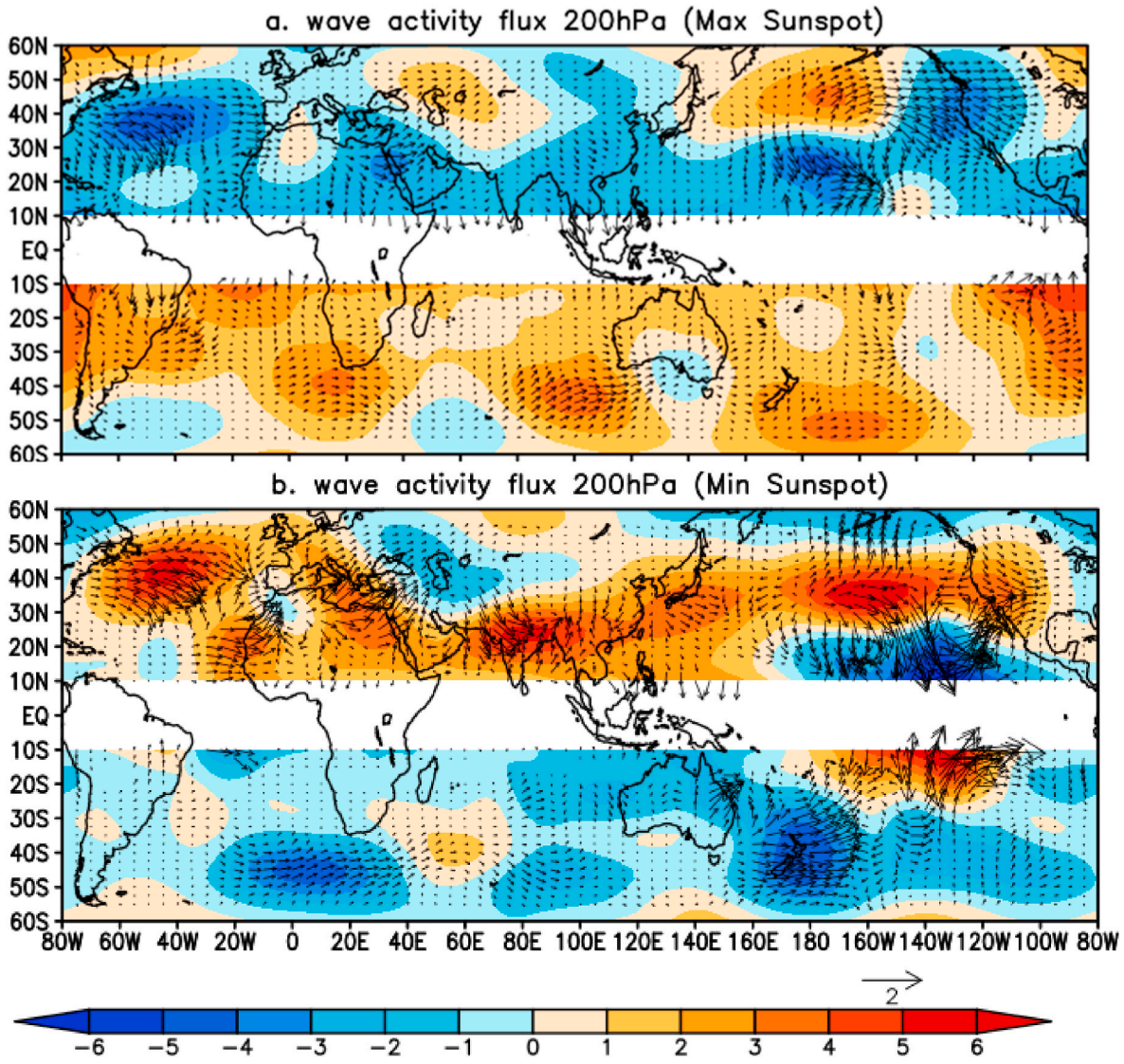

Fig. 9. Time average composite of wave activity flux ($m^2\ s^{-2}$)during (a) maximum sunspot years and (b) minimum sunspot years. Contours shows deviation of 200-hPa mean quasi geostrophic stream function and arrows shows wave activity flux. The white path is the region where quasi geostrophic approximation is neglected.

increased in latent heat flux. During minimum SSN activity (Fig. 6f) indicates more released of latent heat flux over Bay of Bengal. It is important to mention that significant increase in latent heat observed over Arabian Sea, east coastal area along with Indo Gangetic plains and Tibetan plateau regions (Fig. 6f). So, from Fig. 6 it is clear that the during maximum solar activity years high latent heat is available, so more moisture is available for rainfall.

Strong LLJ (Somalian Jet) mainly support the rainfall over Indian region through moisture transport from Arabian Sea and southern Indian Ocean (Findlater, 1969; Naidu et al., 2011). To observe the large scale circulation during maximum and minimum solar activity, time average composite of wind anomalies (vector) along with their magnitude (shaded) at 850 hPa and 200 hPa are shown in Fig. 7. The wind composite at 850 hPa for maximum, minimum and their difference are shown in Fig. 7a, b and 7c; and wind composite at 200 hPa for maximum, minimum and their difference are shown in Fig. 7d, e and 7f respectively. Southwesterly winds with positive magnitude at 850 hPa dominate over most of the Arabian Sea during maximum solar activity (Fig. 7a). Strong LLJ during maximum solar activity years leads to increase the moisture inflow over India, cause more rainfall in Indian landmass (Fig. 7c). Weakening of westerlies leads to the increased strength and extent of TEJ resulting in increasing in moisture and affecting ISMR (Fig. 7e). During the years of minimum solar activity, strong TEJ noticed over Tibetan Plateau, which leading to heavy rainfall in India. This finding support the result presented in Fig. 5, during both years of maximum and minimum, India receives rainfall but mechanism is different. During years maximum solar activity strong LLJ is observed and during years of minimum solar activity, strong TEJ is noticed.

Vertical distribution of Hadley cell circulation is shown for maximum, minimum solar activity years in Fig. 8. An anomalous narrow band of ascending motion in local meridional circulation is seen around 10S to 20N, which afterward becoming descending branch of local Hadley cell between 21N and 38N. It indicate strong circulation over Indian region during maximum solar activity. In case of minimum solar activity, ascending branch of Hadley cell shifts north of equator and two descending branch are observed, indicates weak circulation over Indian landmass. This results support the results presented earlier in this study (Figs. 6 and 7), that during maximum solar activity years, Arabian SST and lhtfl are high, strong Somalian Jet is observed, and strong Hadley cell also lactated, indicating positive rainfall anomaly over north central India. Wave activity flux along with geostrophic stream function at 200 hPa level depicts in Fig. 9 for maximum and minimum solar activity respectively. During maximum solar activity wave train pattern originates from central east Pacific travel towards Atlantic and then to North

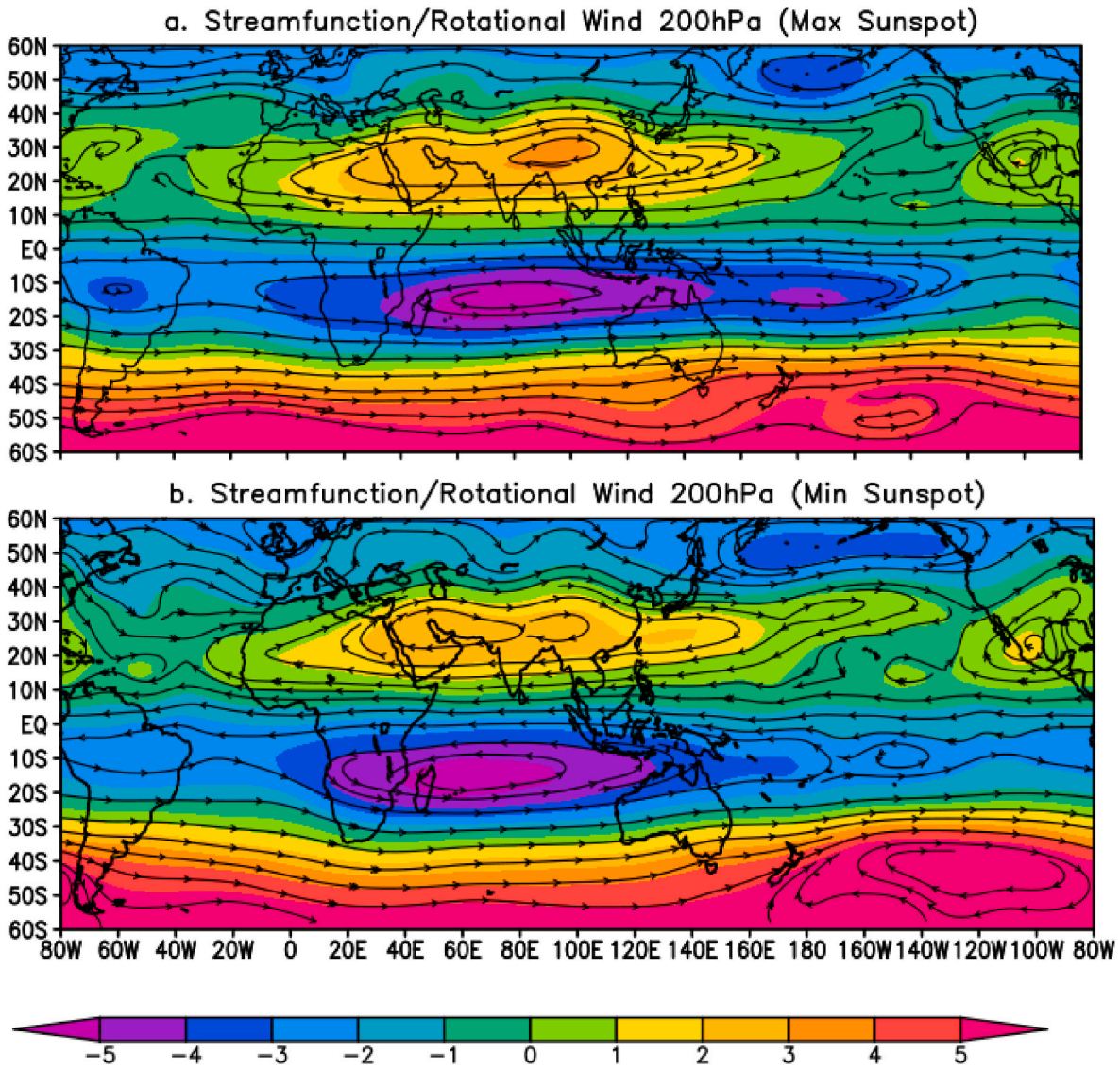

Fig. 10. Time average composite of stream function (s^{-1}) rotational wind (ms^{-1}) at 200 hPa during (a) maximum sunspot years and (b) minimum sunspot years.

Africa (Fig. 9a). In minimum solar activity years, the wave train is more widespread and intense than in maximum solar activity years, wave train pattern originates from North Atlantic Region travel towards North Africa followed by North India and then North east Pacific (Fig. 9b).

Fig. 10 shows stream function and rotational wind at 200 hPa level for maximum and minimum solar activity respectively. During maximum solar activity years intense Tibetan anticyclonic pattern is observed over north of Indian region and during minimum solar activity years the anticyclonic pattern extends westward. Similarly, velocity potential along with divergent wind at 200 hPa is shown in Fig. 11. It is found that the 200 hPa divergence pattern at 10N and 150E gets intense during minimum solar activity years. This result is supported by 200 hPa level temperature composite during minimum solar activity years (Fig. S4), the existence of significant below normal temperature over central Indian region during early-monsoon months (May–June) indicates the presence of high pressure (i.e. divergence) at 200 hPa, which intensifies the TEJ (Fig. S4).

4. Discussions

This study investigates the effect of solar variability on the variability of ISMR through large-scale circulations such as the AMO, IOD, PDO, and Niño 3.4 SST. Previously, it has been noted that during maximum solar activity, stronger tropical monsoon region likely to be exist due to enhanced meridional temperature gradient (Meehl et al., 2003). Furthermore, Scafetta (2010) investigates whether decadal and multi-decadal oscillations have an astronomical basis, and it is discovered that the combined effect of the above natural climate oscillations has caused at least 60% of the global warming recorded since 1970. Varotsos et al. (2014) examined the SST variation and discovered that the SST fluctuations for the time interval between the two SST shifts display 1/f-type longrange correlations, which are common in a wide range of natural systems. Lin et al. (2021), showed that the influence of the solar cycle in central Pacific Ocean is first amplified in the lower stratosphere and then descends to influence the strength of the Hadley circulation in the troposphere and the change in the Hadley circulation then results in the SST footprint in the Northeastern Pacific via surface heat fluxes. Van Loon (2012) observed that during sun spot peak values years stratosphere to surface level climatological means values are increased in Pacific Ocean. Moreover, in recent years, warming of Arabian Sea is observed and it have a potential to alter the monsoon circulation (Ashok et al., 2001), and about 70% of Arabian Sea variability can be explained by AMO (Sun et al., 2019). Therefore, the detail statistical analysis in terms of MODWT, WCA, EMD are carried out for

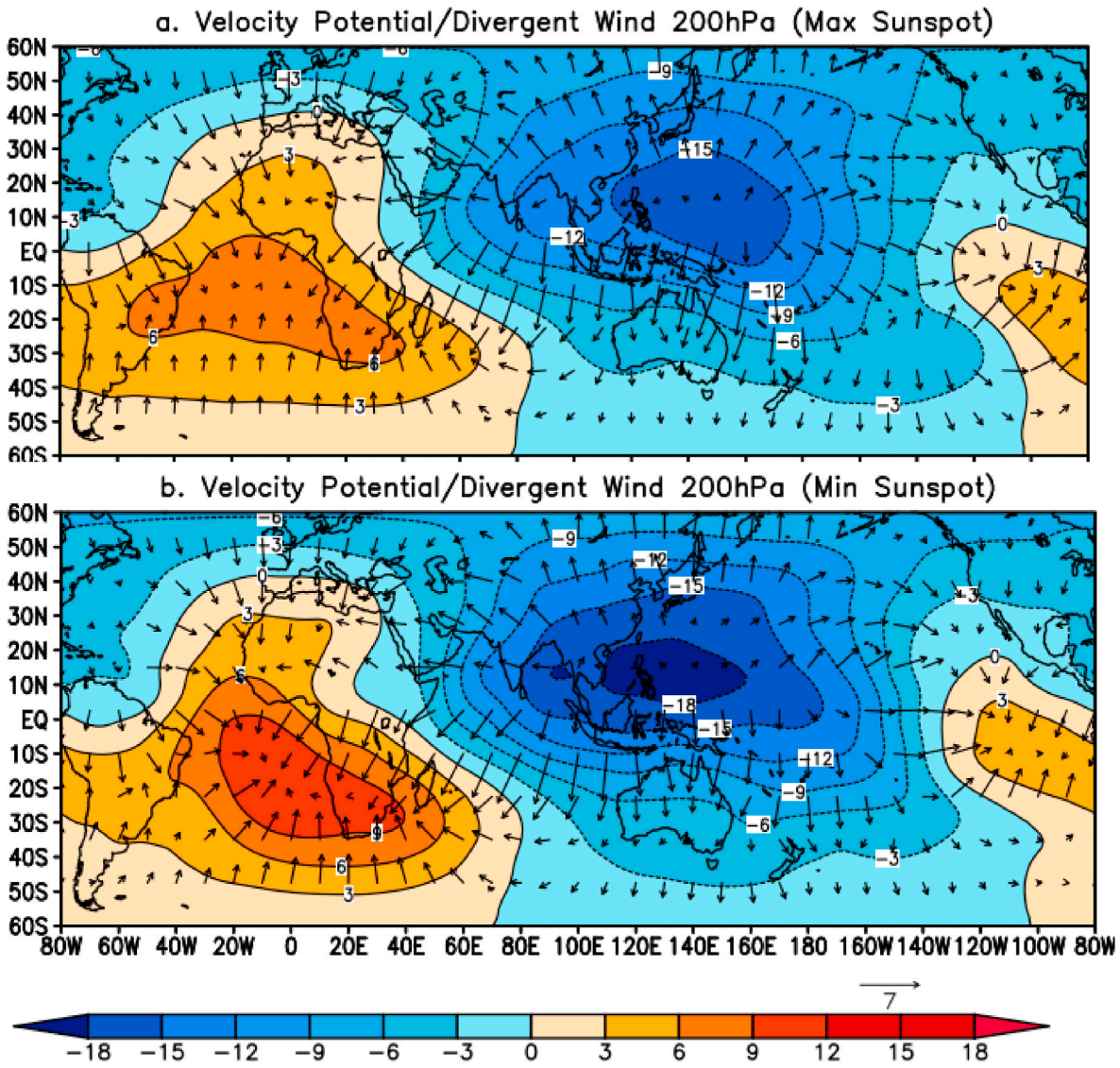

Fig. 11. Time average composite of velocity potential/Divergent wind ($10^6\ m^2 s^{-1}$) at 200 hPa during (a) maximum sunspot years and (b) minimum sunspot years. Positive values shows upper level convergence and negative values shows upper level divergence.

AMO and DMI in this research. Also, the rainfall exhibits intrusive property, the monthly precipitation values and time series revealed persistent long-range power law correlations (the time lags between 4 months and 28 years) when the detrained function method was used for precipitation and rainfall analysis (Efstathiou and Varotsos, 2012; Kantelhardt et al., 2006), while rainfall shows randomness (Efstathiou and Varotsos, 2012).

The mechanism of rainfall during maximum solar activity and minimum solar activity is shown in Schematic diagram (Fig. 12). As mentioned in Fig. S4, during maximum solar activity years, 850 hPa temp over North-west side of India gets intensified during month of May and June. Furthermore, positive lhtfl anomalies in Arabian Sea indicates the presence of ample amount of moisture during summer monsoon season. Strong local Hadley circulation also observed for the maximum solar activity. Strong LLJ carries moisture into the Indian landmass and North India receives ambient rainfall (Fig. 12a). The colder SST anomalies leads to cooler vertical atmospheric column in lower troposphere leading to faster condensation of moisture. At the same time years of solar maxima observed during cold phase of ENSO. This finding shows good collaboration with earlier studies based on solar and climate variability. Roy and Haigh (2012), found that during maximum solar activity years colder temperatures i.e. La Niña-like condition are develop over tropical eastern Pacific and it is well known that during La Niña years, there is higher probability of above normal ISMR (Sikka, 1980; Rajeevan and McPhaden, 2004). Van Loon and Meehl (2012) also noticed the presence of stronger monsoon precipitation during peaks of 11-years solar cycle.

However, in the recent years ENSO-ISMR relation weakening, and IOD is one of the significant ISMR controller. During minimum solar activity, positive SST observed over Arabian Sea. Moreover, positive lhtfl anomalies observed in Bay of Bengal. Also, as mentioned earlier, at 850 hPa level positive temp anomalies are observed over south Indian landmass (Fig. S4). Therefore land-ocean thermal gradient is weakened and Hadley cell associated with monsoon circulation is modified. At 200 hPa strong TEJ is observed during minimum solar activity years (Fig. 12b). Similar type of results shown by Roxy et al. (2015), the increased warming of the Indian Ocean has the potential to weaken the land-sea temperature contrast, shrink the summer monsoon Hadley circulation, and so reduce rainfall across the Indian region. Lee et al. (2009) show that with present-day greenhouse gas and aerosol conditions, the ascending branch of the Hadley cell is enhanced near the equator, and the inter-tropical convergence zone (ITCZ) is shifted

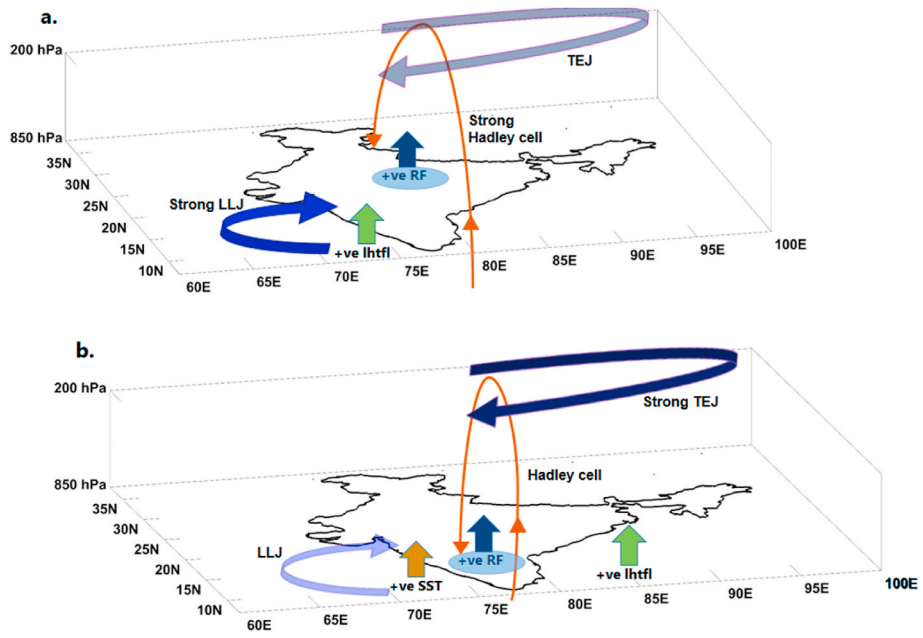

Fig. 12. Schematic Diagram for Indian summer monsoon during (a) maximum SSN and (b) minimum SSN.

northward in response to solar forcing during the boreal winter. From above analysis it may be conclude that during minimum solar activity years, global warming may have surplus radiative heating for ISM.

5. Conclusions

For SSN, ISMR, and large scale circulations in terms of SST indices, the annual variation and 31-year moving mean are analyzed, ISMR does not show direct impact with SSN in terms of significant correlation. The major portion of Arabian Sea come under the 90th percentile of long term mean of surface temperature. Nino 3.4 SST index also checked in context of SSN and ISMR connection.

Through a 31-years moving mean, the DMI has a significant negative correlation with SSN (−0.35) and with ISMR (−0.28). AMO shows a significant positive connection with ISMR (0.68), whereas, Niño 3.4 SST shows significant negative correlation (−0.62) with ISMR. The temporal average composite of ISMR for maximum and minimum solar activity indicates that for both maximum and minimum solar activity, India receives a substantial rainfall, but the mechanisms are entirely distinct. India receives rainfall from a strong LLJ during maximum solar activity years, whilst India receives rainfall from a strong TEJ during minimum solar activity years. The region of influences are also different, during maximum solar activity Northern India receives good amount of rainfall however, and during minimum solar activity Sothern India receives more rainfall. However, year to year variability of ISMR is still remains a study sought to comprehend the impact of solar variability on ISMR variability.

This study also observed same result that during maximum solar activity years, local Hadley cell is enhanced, and strong monsoon circulation is observed. Although this work is based on observational analysis, it also underlined the importance of dynamical analysis for hypothesized mechanisms.

Authors' contribution

VB and JB designed the flow of the research work in discussions with APD. VB carried out the analysis consulting with APD and JB. The manuscript was developed by VB and JB taking input from APD. All authors provide their inputs for revised version. Authors are thankful to Indrani Roy and other reviewer for reviewing our manuscript.

Availability of data

IMD, NCEP-NCAR and World Data Center SILSO, Royal Observatory of Belgium, and Brussels data sets are available on their respective websites.

Availability of code

Code will be available from author on request.

Declaration of competing interest

The authors declare that they have no known competing financial interests or personal relationships that could have appeared to influence the work reported in this paper.

Data availability

Data will be made available on request.

Acknowledgments

Authors are thankful to India Meteorological Department, World Data Center SILSO, Royal Observatory of Belgium, and Brussels for providing observational data sets. Authors are also acknowledge the NCEP-NCAR and NOAA for providing reanalysis data and DMI, PDO and AMO indices. VB acknowledge Director, IIG Mumbai for support.

Appendix A. Supplementary data

Supplementary data related to this article can be found at https://doi.org/10.1016/j.jastp.2023.106134.

References

Agnihotri, R., Dutta, K., Bhushan, R., Somayajulu, B.L.K., 2002. Evidence for solar forcing on the Indian monsoon during the last millennium. Earth and Planetary Science Letters 198 (3–4), 521–527.

Ashok, K., Saji, N.H., 2007. On the impacts of ENSO and Indian Ocean dipole events on sub-regional Indian summer monsoon rainfall. Nat. Hazards 42, 273–285.

Ashok, K., Guan, Z., Yamagata, T., 2001. Impact of the Indian Ocean dipole on the relationship between the Indian monsoon rainfall and ENSO. Geophys. Res. Lett. 28 (23), 4499–4502.
Barde, V., Sinha, P., Mohanty, U.C., Zhang, X., Niyogi, D., 2021. Counter-clockwise epochal shift of the Indian monsoon sparse zone. Atmos. Res. 263, 105806.
Chakravorty, S., Chowdary, J.S., Gnanaseelan, C., 2013. Spring asymmetric mode in the tropical Indian Ocean: role of El Niño and IOD. Clim. Dynam. 40, 1467–1481.
Chaudhuri, S., Pal, J., Guhathakurta, S., 2015. The influence of galactic cosmic ray on all India annual rainfall and temperature. Adv. Space Res. 55 (4), 1158–1167.
Chen, W., Zhou, Q., 2012. Modulation of the Arctic Oscillation and the East Asian winter climate relationships by the 11-year solar cycle. Adv. Atmos. Sci. 29, 217–226.
Chiodo, G., Oehrlein, J., Polvani, L.M., Fyfe, J.C., Smith, A.K., 2019. Insignificant influence of the 11-year solar cycle on the North Atlantic oscillation. Nat. Geosci. 12 (2), 94–99.
Christoforou, P., Hameed, S., 1997. Solar cycle and the Pacific 'centers of action'. Geophys. Res. Lett. 24 (3), 293–296.
Efstathiou, M.N., Varotsos, C.A., 2012. Intrinsic properties of Sahel precipitation anomalies and rainfall. Theor. Appl. Climatol. 109, 627–633.
Findlater, J., 1969. A major low-level air current near the Indian Ocean during the northern summer. Q. J. R. Meteorol. Soc. 95 (404), 362–380.
Gupta, A.K., Mohan, K., Das, M., Singh, R.K., 2013. Solar forcing of the Indian summer monsoon variability during the Ållerød period. Sci. Rep. 3 (1), 2753.
Ghil, M., Lucarini, V., 2020. The physics of climate variability and climate change. Rev. Mod. Phys. 92 (3), 035002.
Ghil, M., 2002. Natural Climate Variability. Encyclopedia of Global Environmental Change.
Gupta, A.K., Das, M., Anderson, D.M., 2005. Solar influence on the Indian summer monsoon during the Holocene. Geophys. Res. Lett. 32 (17).
Haigh, J.D., 1999. A GCM study of climate change in response to the 11-year solar cycle. Q. J. R. Meteorol. Soc. 125 (555), 871–892.
Hathaway, D.H., 2015. The solar cycle. Living Rev. Sol. Phys. 12, 4.
Hiremath, K.M., Mandi, P.I., 2004. Influence of the solar activity on the Indian Monsoon rainfall. N. Astron. 9 (8), 651–662.
Hiremath, K.M., Manjunath, H., Soon, W., 2015. Indian summer monsoon rainfall: dancing with the tunes of the sun. N. Astron. 35, 8–19.
Huang, N.E., Shen, Z., Long, S.R., Wu, M.C., Shih, H.H., Zheng, Q., Yen, N.C., Tung, C.C., Liu, H.H., 1998. The empirical mode decomposition and the Hilbert spectrum for nonlinear and non-stationary time series analysis. Proc. Royal Soc. Lond. Series A: Math. Phys. Eng. Sci. 454, 903–995, 1971.
Hulme, M., Barrow, E.M., Arnell, N.W., Harrison, P.A., Johns, T.C., Downing, T.E., 1999. Relative impacts of human-induced climate change and natural climate variability. Nature 397 (6721), 688–691.
Ineson, S., Scaife, A.A., Knight, J.R., Manners, J.C., Dunstone, N.J., Gray, L.J., Haigh, J. D., 2011. Solar forcing of winter climate variability in the Northern Hemisphere. Nat. Geosci. 4 (11), 753–757.
Kantelhardt, J.W., Koscielny-Bunde, E., Rybski, D., Braun, P., Bunde, A., Havlin, S., 2006. Long-term persistence and multifractality of precipitation and river runoff records. J. Geophys. Res. Atmos. 111 (D1).
Kalnay, E., Kanamitsu, M., Kistler, R., Collins, W., Deaven, D., Gandin, L., Iredell, M., Saha, S., White, G., Woollen, J., Zhu, Y., 1996. The NCEP/NCAR 40-year reanalysis project. Bull. Am. Meteorol. Soc. 77 (3), 437–472.
Krishnamurthy, L., Krishnamurthy, V., 2014. Decadal scale oscillations and trend in the Indian monsoon rainfall. Clim. Dynam. 43, 319–331.
Kumar, K.K., Rajagopalan, B., Cane, M.A., 1999. On the weakening relationship between the Indian monsoon and ENSO. Science 284 (5423), 2156–2159.
Kurths, J., Agarwal, A., Shukla, R., Marwan, N., Rathinasamy, M., Caesar, L., Krishnan, R., Merz, B., 2019. Unravelling the spatial diversity of Indian precipitation teleconnections via a non-linear multi-scale approach. Nonlinear Process Geophys. 26 (3), 251–266.
Langematz, U., Grenfell, J.L., Matthes, K., Mieth, P., Kunze, M., Steil, B., Brühl, C., 2005. Chemical effects in 11-year solar cycle simulations with the Freie Universität Berlin Climate Middle Atmosphere Model with online chemistry (FUB-CMAM-CHEM). Geophys. Res. Lett. 32 (13).
Lee, J.N., Shindell, D.T., Hameed, S., 2009. The influence of solar forcing on tropical circulation. J. Clim. 22 (22), 5870–5885.
Laurenz, L., Lüdecke, H.J., Lüning, S., 2019. Influence of solar activity changes on European rainfall. J. Atmos. Sol. Terr. Phys. 185, 29–42.
Lin, Y.F., Yu, J.Y., Wu, C.R., Zheng, F., 2021. The footprint of the 11-year solar cycle in northeastern pacific SSTs and its influence on the central pacific El Niño. Geophys. Res. Lett. 48 (5) e2020GL091369.
Lindzen, R.S., Nigam, S., 1987. On the role of sea surface temperature gradients in forcing low-level winds and convergence in the tropics. J. Atmos. Sci. 44 (17), 2418–2436.
Lüdecke, H.J., Müller-Plath, G., Wallace, M.G., Lüning, S., 2021. Decadal and multidecadal natural variability of African rainfall. J. Hydrol.: Reg. Stud. 34, 100795.
Maharana, P., Agnihotri, R., Dimri, A.P., 2021. Changing Indian monsoon rainfall patterns under the recent warming period 2001–2018. Clim. Dynam. 57 (9–10), 2581–2593.
Malik, A., Brönnimann, S., 2018. Factors affecting the inter-annual to centennial timescale variability of Indian summer monsoon rainfall. Clim. Dynam. 50 (11–12), 4347–4364.
Meehl, G.A., Washington, W.M., Wigley, T.M.L., Arblaster, J.M., Dai, A., 2003. Solar and greenhouse gas forcing and climate response in the twentieth century. J. Clim. 16 (3), 426–444.
Meehl, G.A., Arblaster, J.M., Matthes, K., Sassi, F., van Loon, H., 2009. Amplifying the Pacific climate system response to a small 11-year solar cycle forcing. Science 325 (5944), 1114–1118.
Mishra, V., Smoliak, B.V., Lettenmaier, D.P., Wallace, J.M., 2012. A prominent pattern of year-to-year variability in Indian Summer Monsoon Rainfall. Proc. Natl. Acad. Sci. USA 109 (19), 7213–7217.
Mohanty, U.C., Raju, P.V.S., Bhatla, R., 2005. A study on climatological features of the Asian summer monsoon: dynamics, energetics and variability. Pure Appl. Geophys. 162, 1511–1541.
Mujumdar, M., Kumar, V., Krishnan, R., 2007. The Indian summer monsoon drought of 2002 and its linkage with tropical convective activity over northwest Pacific. Clim. Dynam. 28, 743–758.
Munz, P.M., Steinke, S., Böll, A., Lückge, A., Groeneveld, J., Kucera, M., Schulz, H., 2017. Decadal resolution record of Oman upwelling indicates solar forcing of the Indian summer monsoon (9–6 ka). Clim. Past 13 (5), 491–509.
Naidu, C.V., Krishna, K.M., Rao, S.R., Kumar, O.B., Durgalakshmi, K., Ramakrishna, S.S. V.S., 2011. Variations of Indian summer monsoon rainfall induce the weakening of easterly jet stream in the warming environment? Global Planet. Change 75 (1–2), 21–30.
Narasimha, R., Bhattacharyya, S., 2010. A wavelet cross-spectral analysis of solar–ENSO–rainfall connections in the Indian monsoons. Appl. Comput. Harmon. Anal. 28 (3), 285–295.
Pai, D.S., Rajeevan, M., Sreejith, O.P., Mukhopadhyay, B., Satbha, N.S., 2014. Development of a new high spatial resolution (0.25× 0.25) long period (1901-2010) daily gridded rainfall data set over India and its comparison with existing data sets over the region. Mausam 65 (1), 1–18.
Peters, D.P., Pielke Sr, R.A., Bestelmeyer, B.T., Allen, C.D., Munson-McGee, S., Havstad, K.M., 2004. Cross-scale interactions, nonlinearities, and forecasting catastrophic events. Proc. Natl. Acad. Sci. USA 101 (42), 15130–15135.
Rajaee, T., Shahabi, A., 2016. Evaluation of wavelet-GEP and wavelet-ANN hybrid models for prediction of total nitrogen concentration in coastal marine waters. Arabian J. Geosci. 9, 1–15.
Rajeevan, M., McPhaden, M.J., 2004. Tropical Pacific upper ocean heat content variations and Indian summer monsoon rainfall. Geophys. Res. Lett. 31 (18).
Ratnam, M.V., Santhi, Y.D., Kishore, P., Rao, S.V.B., 2014. Solar cycle effects on Indian summer monsoon dynamics. J. Atmos. Sol. Terr. Phys. 121, 145–156.
Ropelewski, C.F., Halpert, M.S., 1987. Global and regional scale precipitation patterns associated with the El Niño/Southern Oscillation. Mon. Weather Rev. 115 (8), 1606–1626.
Roy, I., Haigh, J.D., 2012. Solar cycle signals in the Pacific and the issue of timings. J. Atmos. Sci. 69 (4), 1446–1451.
Roy, I., 2014. The role of the Sun in atmosphere–ocean coupling. Int. J. Climatol. 34 (3), 655–677.
Roy, I., Collins, M., 2015. On identifying the role of sun and the El Niño southern oscillation on Indian summer monsoon rainfall. Atmos. Sci. Lett. 16 (2), 162–169.
Roxy, M.K., Ritika, K., Terray, P., Murtugudde, R., Ashok, K., Goswami, B.N., 2015. Drying of Indian subcontinent by rapid Indian Ocean warming and a weakening land-sea thermal gradient. Nat. Commun. 6 (1), 7423.
Sahai, A.K., Grimm, A.M., Satyan, V., Pant, G.B., 2003. Long-lead prediction of Indian summer monsoon rainfall from global SST evolution. Clim. Dynam. 20, 855–863.
Scafetta, N., 2010. Empirical evidence for a celestial origin of the climate oscillations and its implications. J. Atmos. Sol. Terr. Phys. 72 (13), 951–970.
Sikka, D.R., 1980. Some aspects of the large scale fluctuations of summer monsoon rainfall over India in relation to fluctuations in the planetary and regional scale circulation parameters. Proc. Indian Acad. Sci. Earth Planet Sci. 89, 179–195.
Solomon, A., Goddard, L., Kumar, A., Carton, J., Deser, C., Fukumori, I., Greene, A.M., Hegerl, G., Kirtman, B., Kushnir, Y., Newman, M., 2011. Distinguishing the roles of natural and anthropogenically forced decadal climate variability: implications for prediction. Bull. Am. Meteorol. Soc. 92 (2), 141–156.
Solomon, S.C., Liu, H.L., Marsh, D.R., McInerney, J.M., Qian, L., Vitt, F.M., 2019. Whole atmosphere climate change: dependence on solar activity. J. Geophys. Res.: Space Phys. 124 (5), 3799–3809.
Sun, C., Li, J., Kucharski, F., Kang, I.S., Jin, F.F., Wang, K., Wang, C., Ding, R., Xie, F., 2019. Recent acceleration of Arabian Sea warming induced by the Atlantic-western Pacific trans-basin multidecadal variability. Geophys. Res. Lett. 46 (3), 1662–1671.
Takaya, K., Nakamura, H., 2001. A formulation of a phase-independent wave-activity flux for stationary and migratory quasigeostrophic eddies on a zonally varying basic flow. J. Atmos. Sci. 58 (6), 608–627.
Tan, X., Gan, T.Y., Shao, D., 2016. Wavelet analysis of precipitation extremes over Canadian ecoregions and teleconnections to large-scale climate anomalies. J. Geophys. Res. Atmos. 121 (24), 14–469.
Van Loon, H., 2012. Why is the influence of sunspot peaks on the ocean and atmosphere in northern winter seen mainly in the pacific region? Int. Sch. Res. Notices. 2012, 1–5.
Van Loon, H., Meehl, G.A., 2012. The Indian summer monsoon during peaks in the 11 year sunspot cycle. Geophys. Res. Lett. 39 (13).
Van Loon, H., Meehl, G.A., Arblaster, J.M., 2004. A decadal solar effect in the tropics in July–August. J. Atmos. Sol. Terr. Phys. 66 (18), 1767–1778.
Varotsos, C.A., Franzke, C.L., Efstathiou, M.N., Degermendzhi, A.G., 2014. Evidence for two abrupt warming events of SST in the last century. Theor. Appl. Climatol. 116, 51–60.
Walker, J.M., Bordoni, S., Schneider, T., 2015. Interannual variability in the large-scale dynamics of the South Asian summer monsoon. J. Clim. 28 (9), 3731–3750.
Wang, J.S., Zhao, L., 2012. Statistical tests for a correlation between decadal variation in June precipitation in China and sunspot number. J. Geophys. Res. Atmos. 117 (D23).

Webster, P.J., Yang, S., 1992. Monsoon and ENSO: selectively interactive systems. Q. J. R. Meteorol. Soc. 118 (507), 877–926.
Wu, Z., Huang, N.E., Chen, X., 2009. The multi-dimensional ensemble empirical mode decomposition method. Adv. Adapt. Data Anal. 1, 339–372, 03.
Xie, T., Li, J., Chen, K., Zhang, Y., Sun, C., 2021. Origin of Indian ocean multidecadal climate variability: role of the North Atlantic oscillation. Clim. Dynam. 56, 3277–3294.